American Mineralogist, Volume 80, pages 448–453, 1995

H in rutile-type compounds: I. Single-crystal neutron and X-ray diffraction study of H in rutile

R. Jeffrey Swope, Joseph R. Smyth
Department of Geological Sciences, University of Colorado, Boulder, Colorado 80309-0250, U.S.A.
Allen C. Larson
Manuel Lujan Neutron Scattering Center, Los Alamos National Laboratory, Los Alamos, New Mexico 87545, U.S.A.

Abstract

The crystal structure of natural hydrous rutile from a mantle eclogite nodule has been refined from single-crystal neutron diffraction data collected at 24 K. The chemical composition was 95.52 wt% TiO_2, 0.74 wt% Fe_2O_3, 0.68 wt% Al_2O_3, 1.16 wt% Cr_2O_3, 1.86 wt% Nb_2O_5, and 0.04 wt% MnO, with approximately 13000 ppm OH^-, as estimated by IR spectroscopy.

The position of the H atom was located by examining the negative residuals in the difference Fourier maps. The refined position is near the shared edge of the cation octahedron at $x/a = 0.42(1)$, $y/b = 0.50(1)$, and $z/c = 0$ with a site occupancy of 2.7%, which is consistent with the H concentration estimated by IR spectroscopy. The O-H bond distance is 1.05 Å and the OH vector is in the (001) plane, which is consistent with the strong ω-polarization of the OH absorption observed in the IR spectra.

Single-crystal X-ray data were collected from a synthetic anhydrous rutile crystal and a hydrous rutile crystal from the same mantle nodule as the sample used in the neutron study. The detailed X-ray structures of both rutiles were compared and no significant differences were found; the a/c ratios and the O position were identical within error. Therefore, we conclude that the addition of H into rutile for the purpose of charge-balancing excess 3+ cations does not significantly change the structure.

Introduction

Rossman and Smyth (1990) observed that several anhydrous mantle minerals incorporate relatively large amounts of hydroxyl (OH^-) into their structures. These nominally anhydrous minerals may represent a significant reservoir of H_2O in the mantle (Bell and Rossman, 1992). The presence of H_2O can have major effects on phase transitions, including melting relations. Understanding the extent of these potential sources of H_2O requires knowledge of the extent and the mechanisms of OH^- substitution in various anhydrous mantle minerals. Rutile, TiO_2, is a common accessory phase in eclogite and peridotite nodules brought to the surface from the mantle in kimberlitic magmas. Infrared (IR) studies have shown that mantle rutile can contain up to 24000 ppm OH^- (Rossman and Smyth, 1990). Also, rutile is isostructural with the high-pressure phase of SiO_2, stishovite, and may serve as its structural analogue. Recently, Pawley et al. (1993) reported up to 500 ppm OH^- in Al-bearing stishovite.

The purpose of this study is to determine the location of H in rutile and to understand the mechanism of its incorporation into the crystral structure. The crystal structure of natural hydrous rutile from a mantle nodule was refined using single-crystal neutron diffraction data. Neutron diffraction data were used to determine the precise location of H in rutile because H strongly scatters neutrons and only weakly scatters X-rays. The H position was determined by examining the negative residuals in the difference Fourier maps. The refined position lies just off the shared edge of the cation octahedron at $x/a = 0.42(1)$, $y/b = 0.50(1)$, and $z/c = 0$. Additionally, single-crystal X-ray data were collected from a synthetic anhydrous rutile crystal and a crystal from our hydrous mantle rutile. The X-ray data were collected to compare the structural details of anhydrous and hydrous rutile. No significant differences were found in the structural details of these two refinements.

Experimental methods

Neutron diffraction

A single crystal of rutile, approximately 1.0 mm in diameter, was separated from a mantle eclogite nodule. The nodule came from a kimberlitic diatreme at the Roberts Victor Mine, South Africa. Polarized IR studies by Rossman and Smyth (1990) indicate that the rutile in these nodules contains 13000 ppm OH^-. They reported a sharp absorption peak at 3290 cm^{-1} that is strongly polarized in the ω optical plane, indicating that the OH vector lies approximately in the (001) plane. Microprobe analysis shows the chemical composition to be 95.52 wt% TiO_2, 0.74 wt% Fe_2O_3, 0.68 wt% Al_2O_3, 1.16 wt% Cr_2O_3, 1.86

0003–004X/95/0506–0448$02.00

TABLE 1. Neutron and X-ray experimental details for hydrous mantle rutile and synthetic rutile

	Neutron; natural	X-ray; natural	X-ray; synthetic
Space group	$P4_2/mnm$	$P4_2/mnm$	$P4_2/mnm$
Unit cell dimensions			
a (Å)	4.587(2)*	4.5940(2)	4.5922(2)
c (Å)	2.954(2)*	2.9586(2)	2.9574(2)
V (Å^3)	62.15(6)*	62.441(1)	62.367(1)
a/c	1.554	1.5528	1.5528
Crystal dimensions (mm)	1.2 × 1.0 × 0.8	0.1 × 0.1 × 0.1	0.1 × 0.1 × 0.1
Radiation	neutrons (λ = 0.5–5 Å)	Mo$K\alpha$	Mo$K\alpha$
Temperature (K)	24	300	300
Collection limits			
hkl restriction	$(+h, +k, +l)$	$h \geq 0$	$h \geq 0$
Range (sin θ/λ) (Å^{-1})	1.50	1.08	1.08
No. of obs. ($F > 3\sigma$)	940	1500	1495
Data averaging	none		
Laue group		$4/m2/m2/m$	$4/m2/m2/m$
$R_{Av.}$		0.025	0.021
No. unique refl.	246	201	200
Isotropic extinction parameter		0.018(5)	0.42(2)
Refinement			
R_w (%)	0.101	0.016	0.014
No. of parameters	22	11	10

* Unit cell dimensions are extrapolated from X-ray diffraction cell dimensions taken at various temperatures from 300–150 K.

wt% Nb_2O_5, and 0.04 wt% MnO. X-ray diffraction precession photos were taken to rule out twinning and the presence of inclusions.

The crystal was taken to the Los Alamos Neutron Scattering Center (LANSCE) at Los Alamos National Laboratory where it was mounted and optically centered on the single-crystal diffractometer equipped with an Air Products Company Displex refrigerator, model 201. At LANSCE, neutrons are produced by bombarding a W target with a 70-μamp, 20-Hz beam of 800-MeV protons bunched into pulses of 300 ns. The 20-MeV peak spectrum of neutrons produced are then moderated with H_2O to thermal energies. Thus, each pulse has a Maxwellian distribution of neutron energies that peaks at about 1 Å from the room-temperature moderator. For our experiment, neutron wavelengths in the range 0.5–5.0 Å were used. The wavelength of the incident neutron spectra can be determined by the de Broglie relation $E = hc/\lambda$.

The detector on the single-crystal diffractometer at LANSCE is a square (25 cm on a side) two-dimensional position-sensitive ^{3}H-filled proportional counter of the Borkowski-Kopp (1978) design. The x-y position and time-of-flight (TOF), which is the time from the neutron's generation to its detection, are recorded for every neutron detected. The TOF defines the neutron velocity and is directly proportional to its wavelength. The instrument design allows for the collection of a volume of reciprocal space at each setting of the crystal. During the experiment, the crystal remains in a static position for a few hours while one histogram of data is collected. The exposure time, which is dependent on crystal size and neutron-source brightness, is adjusted to obtain adequate counting statistics. Then, the crystal is moved to a new orientation, and the next histogram of data is collected. For rutile, ten histograms were collected to cover the desired portion of reciprocal space, the positive octant ranging to (sin θ)/λ = 1.50 Å^{-1}. The data were collected at 24 K to minimize thermal motion. The instrument was calibrated using data collected from a corundum crystal, a = 4.766, c = 12.996 Å at 298 K. The pertinent details for the neutron data collection are listed in Table 1.

The TOF neutron data were corrected for background and dead time in the detector circuitry and then integrated to yield the set of observed intensities. These observed intensities were corrected for variations in the incident spectra with wavelength. The intensity data from the individual histograms were placed on a common scale using the count in an incident beam ^{235}U fission monitor. The data reduction and structure refinement were carried out using GSAS (General Structure Analysis System, Larson and Von Dreele, 1990), a package of crystallographic and statistical programs designed for reduction of constant wavelength X-ray and TOF neutron diffraction data (single crystal or powder) and structure refinement using the reduced data. The initial values of the atomic positions for this refinement were taken from Shintani et al. (1975). Initially, a scale factor was refined to scale all of the histograms of data. Then, the O position, isotropic displacement factors, and the cation-site occupancy were allowed to vary. Because neutrons are scattered by atomic nuclei, which act as point scatterers, the scattering length of an atom does not vary with d value. Thus, the scattering length for a site is the weighted linear sum of the scattering lengths of the atoms occupying that site. The cation-site occupancy, defined as $(1 - x)$Ti and xFe, was varied to optimize scattering length at the cation site.

Next, a separate scale factor for two of the ten unique histograms of data was varied separately from the scale factor for the other histograms. Finally, the displacement factors were made anisotropic. At this point, difference Fourier sections were calculated and examined for negative peaks at an appropriate distance from O (0.8–1.2 Å).

TABLE 2. Atomic positions and displacement parameters for the rutile refinements

	x/a	y/b	z/c	k	U_{iso}	U_{11}	U_{22}	U_{33}	U_{12}	U_{13}	U_{23}
Neutron (24 K) (hydrous mantle)											
Ti*	0	0	0	1.0	0.0006(5)	0.0006(4)	0.0006(4)	0.0005(5)	−0.0009(4)	0	0
O	0.3045(1)	0.3045(1)	0	1.0	0.0029(3)	0.0028(2)	0.0028(2)	0.0030(3)	−0.0015(2)	0	0
H	0.42(1)	0.50(1)	0	0.027(3)	0.450						
X-ray (300 K) (hydrous mantle)											
Ti′	0	0	0	0.91(5)	0.0063(2)	0.0072(3)	0.0072(3)	0.0045(3)	−0.00008(3)	0	0
Al′	0	0	0	0.08(9)	0.0063(2)	0.0072(3)	0.0072(3)	0.0045(3)	−0.00008(3)	0	0
Nb	0	0	0	0.01	0.0063(2)	0.0072(3)	0.0072(3)	0.0045(3)	−0.00008(3)	0	0
Cr	0	0	0	0.01	0.0063(2)	0.0072(3)	0.0072(3)	0.0045(3)	−0.00008(3)	0	0
O	0.30495(6)	0.30495(6)	0	1.0	0.00528(7)	0.0057(1)	0.0057(1)	0.0044(11)	−0.00211(1)	0	0
X-ray (300 K) (syn. anhydrous)											
Ti	0	0	0	0.992(5)	0.00622(4)	0.00682(8)	0.00682(8)	0.00500(7)	−0.00012(4)	0	0
O	0.30496(8)	0.30496(8)	0	1.0	0.00518(8)	0.0054(1)	0.0054(1)	0.0047(1)	−0.00163(15)	0	0

Note: Ti* represents all octahedrally coordinated cations (Ti 0.96, Nb 0.011, Cr 0.012, Al 0.011, Fe 0.008, Mg 0.003), Ti′ = (Ti + Fe) and Al′ = (Al + Mg).

Each appropriate negative peak was tested by inclusion in the model as a possible H position. Only one of the positions tested maintained a reasonable site occupancy and distance from O; this H position was retained in the final model, which converged with an $R_w = 0.101$ as compared to an $R_w = 0.104$ for the same model without H. The atomic positions and displacement parameters are listed in Table 2. Selected bond distances and angles are listed in Table 3. The unit cell dimensions obtained from the neutron diffraction data were used only for determination of diffraction peak locations in the integration. The unit cell dimensions used for all other calculations were obtained by exploration of X-ray cell dimensions measured at various temperatures from 24 to −150 °C. Figure 1 shows the X-ray unit cells and the original and adjusted neutron unit cell dimensions.

X-ray diffraction

X-ray data were obtained from small (100 μm in diameter) equant rutile crystals: one synthetic, nominally anhydrous rutile crystal (with only 60 ppm OH^-) supplied by G. R. Rossman, and one hydrous rutile crystal from the same mantle nodule as the neutron sample. The crystals were mounted on a Siemens four-circle diffractometer equipped with a rotating Mo target, an 18-kW generator, and a graphite monochromator. Unit cell dimensions were calculated from the least-squares refinement of 35 high-angle reflections, ranging in 2θ from 70–80°. Variable speed continuous θ-2θ scans were used with the scan rate restricted to 2–20 °/min for the anhydrous and 15–30 °/min for the hydrous rutile. A hemisphere of intensity data was collected for each crystal out to $(\sin\theta)/\lambda = 1.08$ with the generator operating at 50 kV and 250 mA. For the anhydrous rutile, 1495 reflections (including standards) were measured, of which 200 with intensities 2σ above the background were unique. For the hydrous rutile, 1501 reflections (including standards) were collected, of which 201 with intensities 2σ above the background were unique. The details of the X-ray data collections are given in Table 1.

The data collected for the anhydrous and the hydrous crystals were corrected for background and then integrated to yield a set of observed intensities for each. The intensity data were corrected for Lorentz and polarization effects. An analytical absorption correction failed to improve the final R in either model probably because both crystals are equant and small. Therefore, an absorption correction was not used. The structure refinements were carried out using SHELLXTL (Siemens, 1989). The initial atom positions and displacement parameters were taken from Shintani et al. (1975). Site occupancies of Ti′ = (Ti + Fe) and Al′ = (Al + Mg) were allowed to vary; however, Nb and Cr were fixed to agree with the chemistry obtained from microprobe analysis. Initially, the scale factor and the O position were varied. Isotropic displacement factors and an extinction parameter were then added. Finally, the displacement factors were made anisotropic resulting in a final $R = 0.014$ for the anhydrous and $R = 0.016$ for the hydrous rutile. The atom positions and displacement parameters for both refinements are listed in Table 2. Selected bond lengths and angles are listed in Table 3.

TABLE 3. Selected interatomic distances and angles for the rutile refinements

	Neutron (24 K) hydrous mantle	X-ray (300 K) hydrous mantle	X-ray (300 K) Syn. anhydrous
Ti*-O	1.9763(1)	1.9812(6)	1.9805(8)
-O	1.9467(1)	1.9479(6)	1.9470(8)
O-O	2.5373(2)	2.535(1)	2.533(1)
-O	3.3212(2)	3.326(1)	3.325(1)
-H	1.05(4)		
-H	1.56(4)		
O-H···O	154.3(3)		

Note: Ti* represents all octahedrally coordinated cations (Ti 0.96, Nb 0.011, Cr 0.012, Al 0.011, Fe 0.008, Mg 0.003).

DISCUSSION

The rutile structure (Fig. 2) is composed of distorted cation octahedra interconnected by the sharing of corner

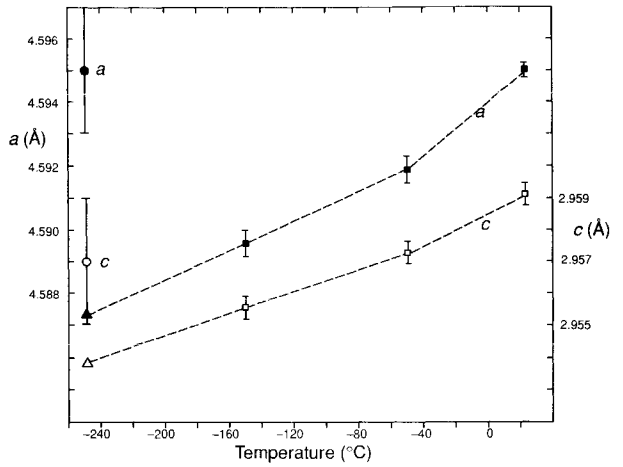

Fig. 1. X-ray (squares) and neutron (circles) cell parameters measured at various temperatures (a = solid, c = open). The cell parameters at −250 °C (triangles) are simple linear extrapolations through the X-ray cell edges at −50 and −150 °C. The uncertainties in these parameters are large enough to accommodate any reasonable nonlinearity owing to diminished thermal expansion at low temperature.

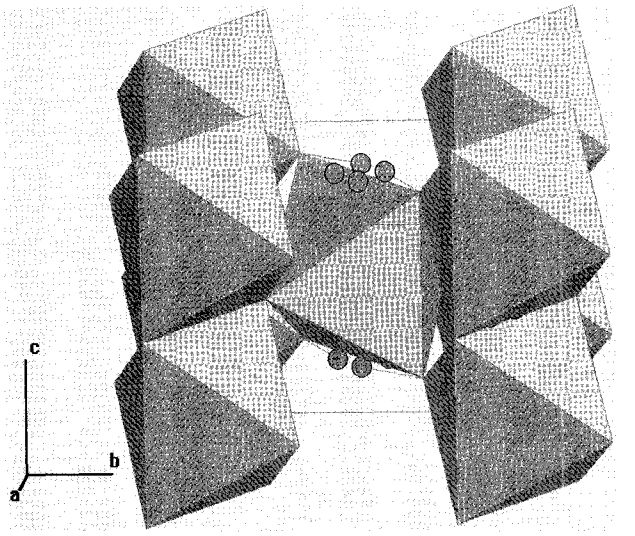

Fig. 2. Polyhedral representation of the rutile structure showing the position of the H atoms (circles) slightly off the shared octahedral edge. Approximately 2% of the O atoms in the structure are OH^-, thus all four H positions would never be occupied simultaneously. Only H positions completely within the unit cell are shown.

and edge O atoms. Each octahedron is elongated along an axis passing through opposite corners, resulting in two longer and four shorter cation-O bonds. The octahedra share edges to form octahedral chains, which run parallel to the **c** axis. Within a chain, each octahedron is positioned with its long axis perpendicular to the length of the chain. Each chain is linked to four adjacent chains by sharing corner O atoms. Adjacent chains are shifted ½ c and rotated 90° around the **c** axis (chain axis) relative to each other. This arrangement leaves O in trigonal planar coordination with respect to cations, with one longer and two shorter cation-O bond distances. The O-O distance along the shared edge within the chain is much shorter than the unshared edges of the octahedra.

Rutile commonly contains small amounts of H, which serve to charge-balance an excess of 3+ cations not compensated by 5+ cations. Hammer and Beran (1991) examined variations in the OH^- concentrations of rutiles from various geological environments. The H_2O^+ concentration estimated from IR spectra ranged from 0.04 to 0.21 wt%. All samples showed a sharp absorption feature at 3280 cm^{-1}. Hammer and Beran (1991) concluded that OH^- concentrations in rutile are predominantly a function of the activity of the hydrous components during crystallization; OH^- concentrations only weakly correlate with the concentration of excess 3+ cations because excess 3+ cations can also be compensated by structural defects. Vlassopoulos et al. (1993) also examined naturally occurring rutiles using IR spectroscopy. They investigated the role of H in rutile in comparison with other impurities and also concluded that H is present to compensate for 3+ cations (Cr, Fe, V, Al) that are only partially compensated by 5+ cations (Nb, Ta). Additionally, they discussed the possibility of using rutile as a geohygrometer.

Johnson et al. (1968) used energy calculations to identify two possible sites for H in rutile: (½,0,0) and (½,½,0). These calculations indicate that the (½,½,0) position is energetically favored. However, the difference between the energies calculated for the sites was too small to be definitive. Additionally, Johnson et al. (1968) calculated the vibrational energy levels for a proton in a double-well potential for the two possible H positions and compared them with IR spectra. They concluded that (½,0,0) was the most likely position for H. Andersson et al. (1973, 1974) and Ohlsen and Shen (1974) investigated Fe-doped rutile containing H using electron spin resonance (ESR) and IR spectroscopy. They concluded that H located at (½,0,0) is consistent with their results.

In rutile, strong ω-polarization of the sharp IR absorption, first reported by Soffer (1961), results from O-H stretching and indicates that the OH vector is approximately in the (001) plane. In the (001) plane there are two possible sites for H, one near (½,0,0) and another near (½,½,0). Beran and Zemann (1971) concluded, on the basis of polarized IR results and in part on the correlation of the O-H···O bond distance with the wave number of the O-H stretching mode (Nakamoto et al., 1955), that H probably resides near the (½,0,0) position. Figure 3, adapted from Nakamoto et al. (1955), shows that the absorption feature for a straight O-H···O bond distance of 2.8 Å occurs at a wave number of 3280 cm^{-1}. In the (001) plane of rutile the O-O distance across the (½,0,0) position is 3.33 Å, whereas it is only 2.53 Å across the (½,½,0) position. If the O-H···O bond were straight

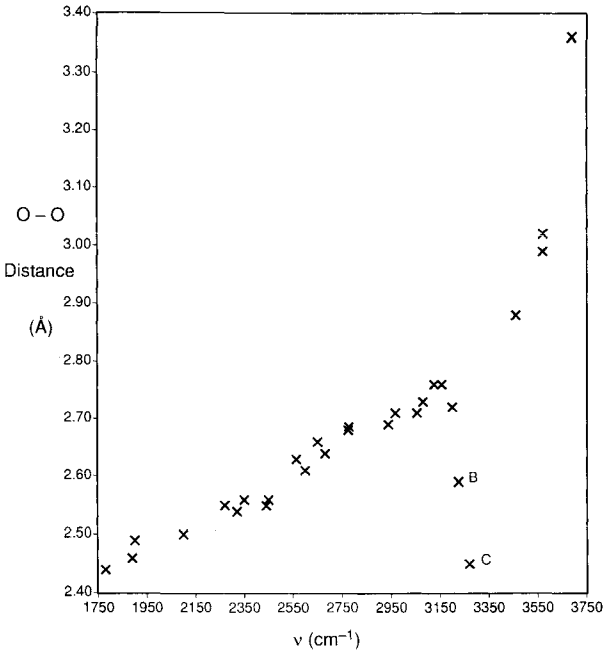

Fig. 3. O-H stretching frequency ν vs. O-O distance for O-H $\cdots$O bonds after Nakamoto et al. (1955). Points B and C are for nonlinear O-H$\cdots$O bonds, whereas all other points are for linear O-H$\cdots$O bonds.

in rutile, the OH^- absorption frequency corresponding to a straight H bond of 2.53 Å would be much lower than the observed 3280 cm^{-1}, suggesting that H sits near the (½,0,0) position. However, according to Nakamoto et al. (1955), bending the O-H$\cdots$O bond dramatically increases the O-H stretching frequency for any particular O-H $\cdots$O distance (shown by points B and C in Fig. 3), suggesting that (½,½,0) might also be a viable position for H.

In this study of hydrous mantle rutile, the H position at $x/a = 0.42(1)$, $y/b = 0.50(1)$, and $z/c = 0$ with an O-H bond distance of 1.05 Å and a site occupancy of 2.7% was located and refined using single-crystal neutron data. The difference Fourier maps were carefully examined for negative scattering from H near (½,0,0), but no such feature was found. The limited concentration of H, the small size of the crystal, and the limited collection time combined to make the H position difficult to locate in the Fourier maps. However, the H position refined with good precision, with a site occupancy in agreement with the IR estimates of H concentration, and including H in the structure model reduced the model *R*. Moreover, the refined OH^- vector is in the (001) plane, which is consistent with the strong ω-polarization of the IR absorption. The neutron refinement shows that the O-H$\cdots$O bond is bent with an angle of 154.3°, allowing for a higher O-H stretching frequency than would be predicted considering the short O-H$\cdots$O bond distance of 2.53 Å. Additionally, the refined H position seems reasonable on the basis of crystal-chemical considerations because H located close to the shared edge should partially mitigate the O-O repulsion across that edge. Our results do not rule out the possibility that other H positions with smaller site occupancies exist in rutile; however, they do indicate that $x/a = 0.42(1)$, $y/b = 0.50(1)$, and $z/c = 0$ is the dominant H position in hydrous mantle rutile at atmospheric pressures. Stishovite (SiO_2) is isostructural with rutile, has been shown to contain H, and has an even shorter shared edge (Pawley et al., 1993). Therefore, it seems reasonable to expect that the H position in stishovite is also located near the shared edge in the (001) plane.

The structural details of the X-ray refinements in Tables 1, 2, and 3 show no significant differences; the O position, the bond angles, and the a/c ratio are the same within error. The displacement factors are also virtually the same for both refinements. The only difference between the two refinements is that the hydrous rutile has slightly larger unit cell dimensions than the anhydrous rutile. This simply reflects the presence of larger cations (such as Fe) in the hydrous rutile. Apparently the addition of small amounts of structurally bound H to the rutile does not significantly affect the structural details.

Acknowledgments

This study was funded by U.S. Department of Energy Office of Basic Energy Sciences grant DE-FG02-92ER14233 to J.R.S. and by Los Alamos National Laboratory operated by University of California under grant no. W-7405-ENG-36 from the U.S. Department of Energy. The authors thank G.R. Rossman for contributing IR results and the synthetic rutile sample. We also thank T.C. McComick for assisting in the low-temperature X-ray cell determinations and J. Munoz for constructive review of the manuscript.

References cited

Andersson, P.-O., Kollberg, E.L., and Jelenski, A. (1973) Extra EPR spectra of iron-doped rutile. Physical Review B, 8, 4956–4965.

——— (1974) Charge compensation in iron-doped rutile. Journal of Physics C: Solid State Physics, 7, 1868–1880.

Bell, D.R., and Rossman, G.R. (1992) Water in the Earth's mantle: The role of nominally anhydrous minerals. Science, 255, 1391–1397.

Beran, A., and Zemann, J. (1971) Messung des Ultrarot-Pleochroismus von Mineralen: XI. Der Pleochroismus der OH-Streckfrequenz in Rutil, Anatas, Brookit und Cassiterit. Tschermaks mineralogishe-petrographische Mitteilungen, 15, 71–80.

Borkowski, C.J., and Kopp, M.J. (1978) Recent improvements to R-C line encoded position-sensitive proportional counters. Journal of Applied Crystallography, 11, 430–434.

Hammer, V.M.F., and Beran, A. (1991) Variations in the OH concentration of rutiles from different geological environments. Mineralogy and Petrology, 45, 1–9.

Johnson, O.W., Ohlsen, W.D., and Kingsburg, P.I. (1968) Defects in rutile: III. Optical and electrical properties of impurities and charge carriers. Physical Review, 175, 1102–1109.

Larson, A.C., and Von Dreele, R.B. (1990) Los Alamos National Laboratory, General Structure Analysis System (GSAS). LA-UR 86-748, Los Alamos, New Mexico.

Nakamoto, K., Marghoshes, M., and Rundle, R.E. (1955) Stretching frequencies as a function of distance in H bonds. Journal of the American Chemical Society, 77, 6480–6488.

Ohlsen, W.D., and Shen, L.N. (1974) Hyperfine structure of Fe^{3+} ions in rutile (TiO_2). Journal of the Physical Society of Japan, 37, 1467.

Pawley, A.R., McMillan, P.F., and Holloway, J.R. (1993) H in stishovite with implication for mantle water contents. Science, 261, 1024–1026.

Rossman, G.R., and Smyth, J.R. (1990) Hydroxyl contents of accessory minerals in mantle eclogites and related rocks. American Mineralogist, 75, 775–780.

Shintani, H., Sato, S., and Saito, Y. (1975) Electron-density distribution in rutile crystals. Acta Crystallographica, B31, 1981–1982.

Siemens, Inc. (1989) SHELLXTL, Siemens Analytical X-ray Instruments, Inc., Madison, Wisconsin.

Soffer, B.H. (1961) Studies of the optical properties and infrared absorption spectra of rutile single crystals. Journal of Physical Chemistry, 35, 940.

Vlassopoulos, D., Rossman, G.R., and Haggerty, S.E. (1993) Coupled substitution of H and minor elements in rutile and the implications of high OH contents in Nb- and Cr-rich rutile from the upper mantle. American Mineralogist, 78, 1181–1191.

Manuscript received March 28, 1994
Manuscript accepted February 8, 1995